Title
SUPERBEFORMATION AND SOME NEW RESULTS MITH HERA

Author
Diamond, R.M.

Publication Date
1988-10-01

Lawrence Berkeley Laboratory
UNIVERSITY OF CALIFORNIA

Presented at the 20th International Summer School on Nuclear Physics, Mikolajki, Poland, September 2–11, 1988

Superdeformation and Some New Results with HERA

R.M. Diamond

October 1988

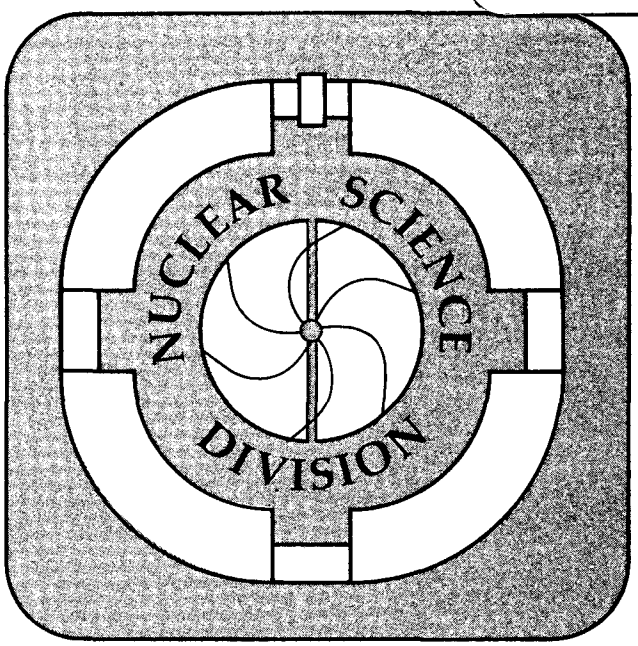

Prepared for the U.S. Department of Energy under Contract Number DE-AC03-76SF00098.

DISCLAIMER

LBL-26149

Superdeformation, and Some New Results with HERA

R.M. Diamond

Nuclear Science Division
Lawrence Berkeley Laboratory
1 Cyclotron Road
Berkeley, California 94720

October 1988

This work was supported by the Director, Office of Energy Research, Office of High Energy and Nuclear Physics, Nuclear Physics Division of the of the U.S. Department of Energy under Contract DE-AC03-76SF00098.

SUPERDEFORMATION, AND SOME NEW RESULTS WITH HERA

R. M. DIAMOND
Nuclear Science Division, Lawrence Berkeley Laboratory

I am grateful to the organizers for the opportunity to take part in this twentieth jubilee meeting of the Mikołajki Summer School on Nuclear Physics, and I want to wish them another twenty years of equally successful, enjoyable, and instructive schools and a wonderful semi-jubilee meeting then.

As you all know, in-beam γ-ray spectroscopy has had an outpouring of new experiments, new ideas, new results in the last few years. On the experimental side, a major reason has been a technical development, the construction of multi-detector, Compton-suppressed Ge arrays. Our array, HERA, which was the first to employ bismuth germanate (BGO) shields as Compton suppressors (Diamond and Stephens 1981), consists of 21 Ge detectors around a $\sim 4\pi$ central ball of BGO sectors. Figure 1 shows the

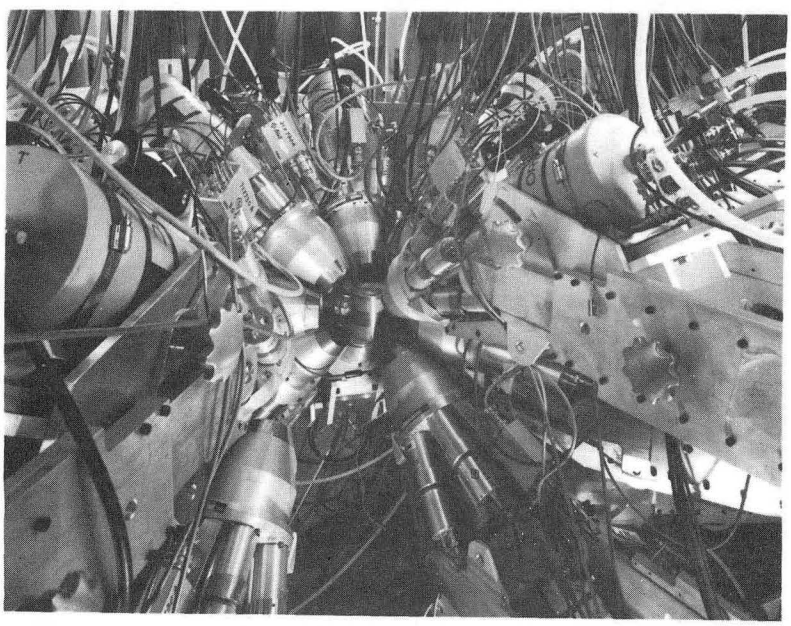

CBB 853-2061

Fig. 1. The 21-element, Compton-suppressed Ge array, HERA, viewed from the opened side.

actual array of Ge detectors when it was completed in early 1985. During the present month (September) the 40 BGO sectors of the central ball are being installed to complete the system. The goal of an array is to achieve the best statistics and the highest resolving power possible. For the former purpose one needs as many detectors covering as large a solid angle as one can fit around the target and can pay for. The latter goal, the ability to isolate a particular γ-ray cascade, also depends upon the number of detectors through the number of coincident gates required to achieve the desired separation. When dealing with a singles spectrum (or independent γ rays) we cannot do better than the Ge resolution. But for complex cascades one may gain roughly an order of magnitude better separation for each gate used. Figure 2a shows a 60 keV long section of a γ-ray spectrum containing 1 γ ray each (energies chosen at random) from 20 cascades (In rare-earth rotational cascades, the difference between consecutive transitions is ~ 60 keV). The energy resolution of the detector is taken to be 3 keV so there are 20 resolvable bins in the spectrum. With no other information we cannot resolve further this spectrum and decide whether the degenerate lines

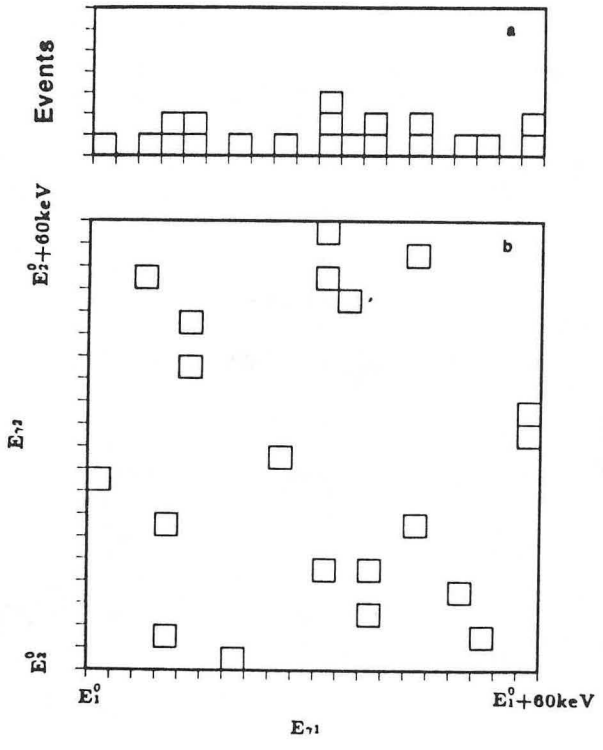

Fig. 2. Schematic drawing of a) 60 keV section of a singles spectrum from 20 rotational cascades, and b) a corresponding section of a coincidence matrix from the same rotational cascades.

come from a repeat of the same cascade or not. But a second coincident detector viewing these cascades would produce the two-dimensional matrix shown in Fig. 2b. There are now 20^2 or 400 resolvable points and the original 20-count spectrum resolves into 20 individual cascades. This type of increase in effective resolution has been known for many years and $\gamma\gamma$ coincidence spectra can be obtained that are much cleaner than

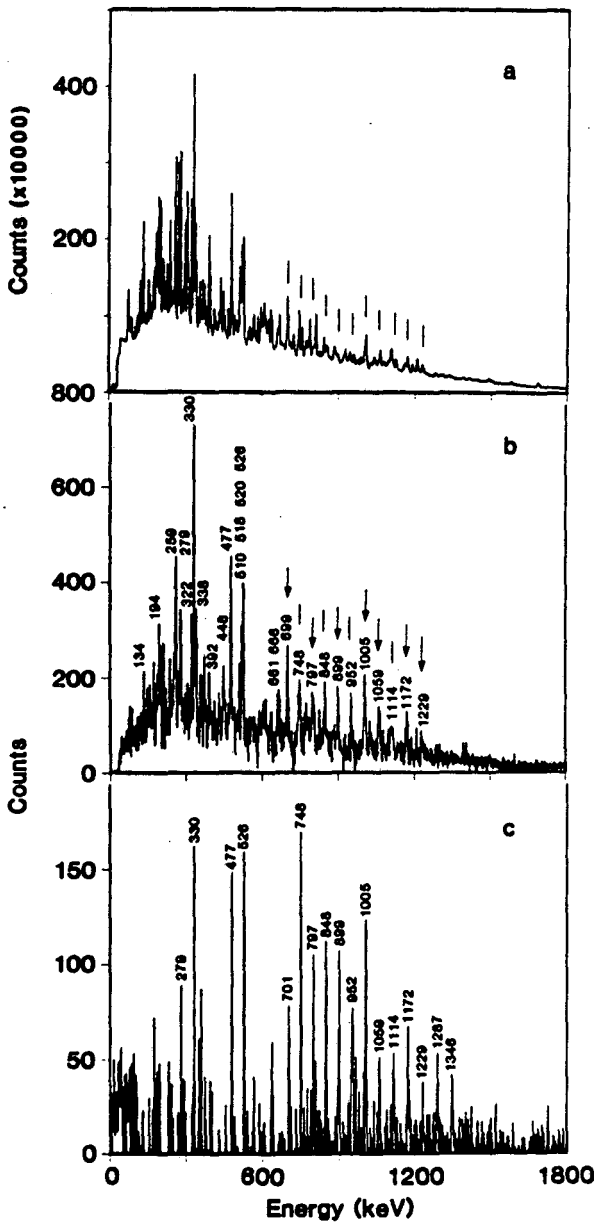

Fig. 3. a) "Singles" spectrum from the reaction $^{29}Si + ^{124}Sn$; the position of lines from the SD band in ^{148}Gd are marked. b) Sum of spectra (single-) gated on three of the cleanest SD lines. Lines marked by arrows are double (in this or a neighboring nucleus). c) Spectrum summed over all double-gate combinations of ten lines in the SD band, (Deleplanque et al., 1988).

a singles spectrum. However, in a complex decay scheme today there may be 200 or more transitions and more than half may be degenerate, so that still greater resolving power is needed. This can be achieved by considering still higher coincidence folds, e.g., triple coincidence (double-gated) spectra, to increase further the number of resolvable bins. In our example the triples matrix would have 20^3 or 8000 resolvable points. To show you that this is not just an academic argument, I give you an example involving the subject I shall discuss in the remainder of these two lectures, namely, superdeformed bands.

The top of Fig. 3 shows a pseudo-singles in-beam spectrum from the reaction of 150 MeV ^{29}Si on ^{124}Sn. It is a total projection of the three- and higher-fold data, and so is cleaner than a true singles spectrum. The tallest line is a 330 keV transition, a $16^+ \rightarrow 14^+$ transition that represents the total ^{148}Gd intensity. The superdeformed (SD) band in this nucleus has transitions in the energy range 700-1300 keV (shown by the vertical lines) and we now know that they have an intensity of order 200 times weaker than that of the 330 keV line (Deleplanque et al., 1988). Obviously they cannot be observed in this spectrum. But if by some means we can determine the energies of some of the SD transitions, we can use them as gates to give a better resolved spectrum. The middle spectrum in the figure shows the result of the sum of three gates on relatively clean SD lines. Now a band is visible, but the transitions marked with arrows are all double and it is these non-SD components that are contributing mainly to the 330 keV line. Still, by going to $\gamma\gamma$ coincidences, the ratio of the average intensities of the SD transitions to that of the 330 keV line has improved by more than an order of magnitude. The bottom spectrum shows what happens if three-fold coincidences are used; it is the sum of spectra obtained from pairs of gates on ten of the expected SD band transitions. The clean-up of the spectrum is now complete. The relative intensities of the SD lines to that of the 330 keV line is ~1:1 (after correction for efficiencies), an improvement with two gates by a factor of 200 over the top spectrum. For more complex spectra, four- and higher-fold spectra will be useful, and for this and other reasons still higher coincidences are the goal in the planning for the next generation of Ge arrays, e.g., GAMMASPHERE and Euroball.

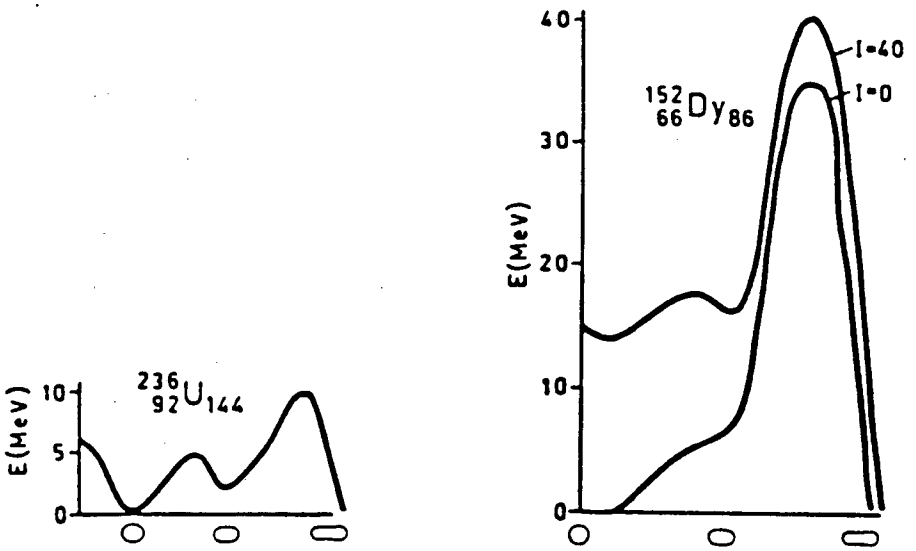

Fig. 4. Schematic, one-dimensional fission barrier for ^{236}U(left) and ^{152}Dy(right). Addition of high-spin rotational energy decreases the slope, making possible the development of a second minimum in the ^{152}Dy system also (Åberg et al., 1988).

Let us now get on with the topic of superdeformation. Because this is a school and not a conference, I shall start by giving a brief history of how this subject developed. The story starts more than 25 years ago when Polikanov and his colleagues (1962) discovered the spontaneously fissioning isomers in some actinide nuclei. These were low-lying, low-spin isomeric states that decayed with spontaneous fission half-lives orders of magnitude smaller than expected from the existing systematics. It was several years before Strutinski (1967) gave the explanation; these were (prolate) shape isomers with one axis twice as long as the other two, and they existed in a secondary minimum in the potential energy surface (Fig.4, left). Fission from such states involved tunneling through a much thinner potential barrier and starting at a higher energy than for normal states in the first minimum. It is the (increasingly) large Coulomb potential in these high-Z nuclei that opposes the nuclear surface tension, providing a nearly level potential energy surface and thus permitting the existence of a secondary well. Such low-spin shape isomers would not be possible lower in the Periodic table where the smaller Coulomb energy leads to a much higher fission barrier and steeper slope. But theoreticians already predicted years ago (Neergaard et al., 1976), Ragnarsson et al., 1980, Åberg et al., 1988 and many others) that the centrifugal potential at high spin for lower Z nuclei would add to the Coulomb potential and help level the potential energy surface to again allow the existence of secondary wells, as shown in Fig. 4, right. But

what causes these secondary dips? They are shell effects due to the bunching of nuclear levels. In an anisotropic harmonic oscillator potential, there are additional shell gaps beyond the spherical ones when the axes' lengths are in the ratios of simple integers (meaning that the nucleonic orbits have simple degeneracies), Fig. 5 (Bohr and Mottelson, 1975). In such a potential, the next most important shell gaps after the spherical ones are those associated with 2:1 axis ratios. Better calculations using Nilsson or Woods-Saxon potentials have produced more realistic total potential energy surfaces (Fig. 6), and although the 2:1 ratio still confers special stability at certain proton and neutron numbers, chains of gaps are predicted to occur with changes in the nucleon number (Dudek et al., 1987, and others). These have varying axial ratios, ranging downward from the 2:1 "superdeformed" case to near "normal" deformation, but also going to still longer shapes, such as the not yet observed "hyperdeformed" 3:1 axial ratio.

We can learn a great deal from a study of SD bands and their properties. As mentioned above, from the nature of the potential energy surface these bands must occur in moderate Z nuclei at high spin, and so their behavior tells us about nuclei under different conditions than with the usual low-spin bands. Centrifugal and Coriolis forces are large, pairing

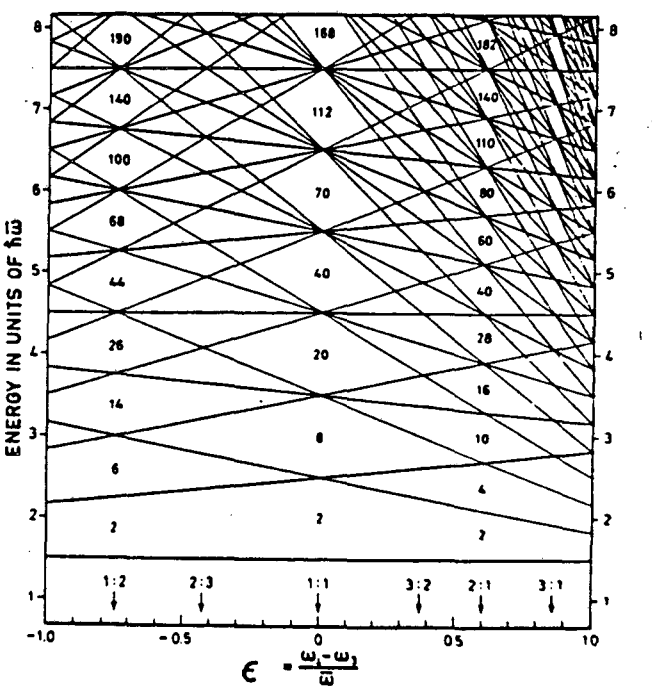

Fig. 5. Single-particle spectrum for axially symmetric, harmonic oscillator potential. Arrows mark deformations corresponding to the

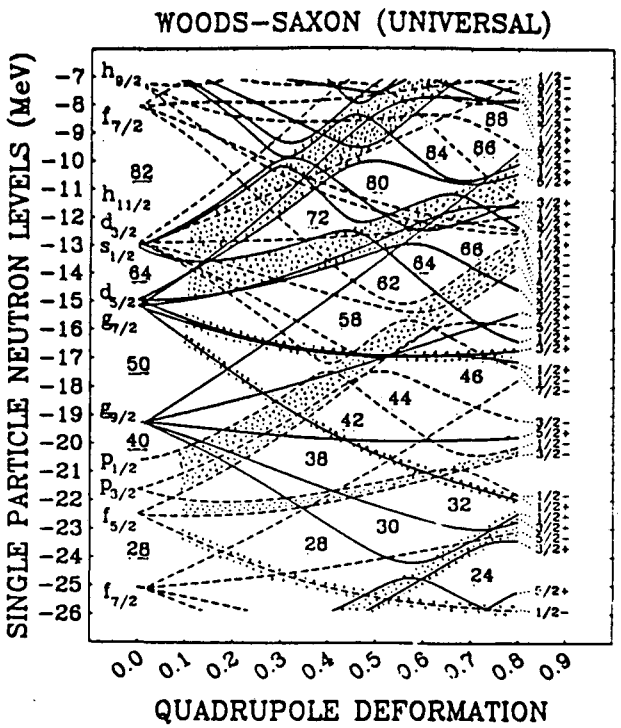

Fig. 6. Single-particle spectrum on a realistic nuclear potential. Higher level-density regions are shaded (Dudek et al., 1987).

correlations are reduced, low-Ω, high-j orbitals from one and two shells above the Fermi surface for spherical shapes drop down and become the dominant orbitals in the nuclear configuration. The systematics of their occurrence will tell us about the location and strength of non-spherical shell gaps and allow conclusions on the "goodness" of different calculations.

Indications of the existence of such a 2:1 SD band was given in a continuum γ-ray study (Nyako et al., 1984) of ^{152}Dy by the observation in the two-dimensional coincidence matrix of ridges on either side of the diagonal valley that were closer together than expected for normal bands. But the spectacular breakthrough occurred just over two years ago when a group at Daresbury found 19 discrete members of a SD band in ^{152}Dy that cascaded from about spin 60 ℏ to ~ 24 ℏ, Fig. 7 (Twin et al., 1986). The intensity of the band increases down to about spin 46 ℏ and then remains constant at ~ 1% of the total yield of ^{152}Dy. Around spin 26 ℏ the intensity falls sharply; the band disappears in a couple of transitions. This discovery answered the question of whether the theoreticians had been right or not, and the 1% intensity explained why the band could not be found until Ge arrays had been constructed to give adequate sensitivity. But the properties of the band raised many new

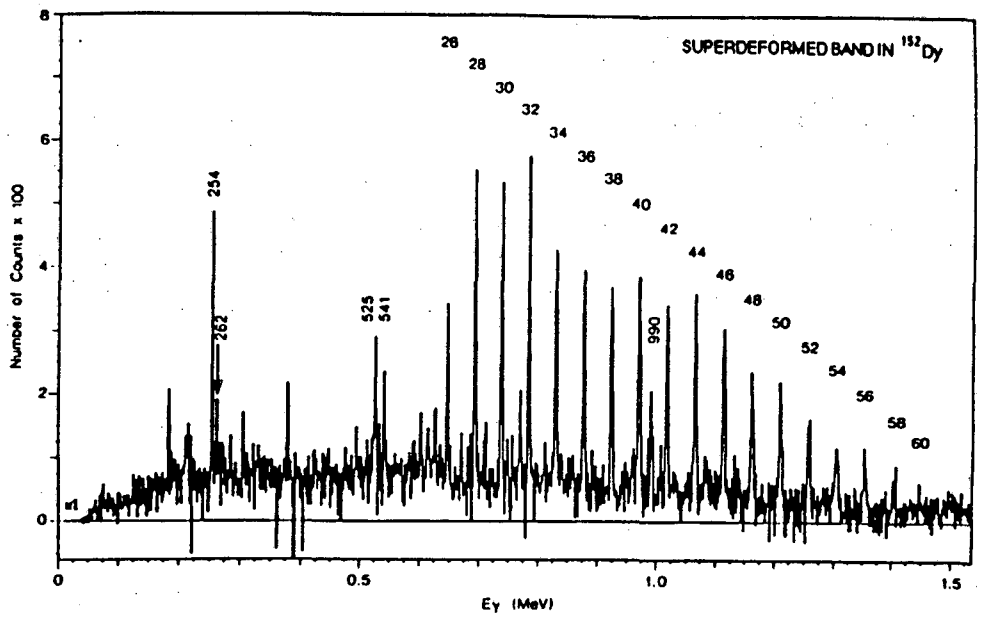

Fig. 7. Coincidence spectrum of ^{152}Dy band (Twin et al., 1986).

questions, and most of them have not really been answered as yet. For example, the SD band at its start around spin 60 $\hbar$ is ~ 20 times more intense than the extrapolation of the intensities of known discrete normal bands to such a high spin (none have been observed that high). Still another mystery is why and how the SD band ends so suddenly with the intensity vanishing in two transitions. Another question is why no trace could be found of the transitions linking it to the yrast states to which it decayed. Or why the SD band apparently decays entirely to the somewhat oblate main band of single-particle states rather than to the normally deformed, prolate band which parallels it. One can also wonder why only one discrete band is seen, although higher-lying excited bands must exist to give the extra intensity we have observed in the ridges of the two-dimensional matrix when this band is produced in a different reaction, ^{40}Ar + ^{116}Cd (deVoigt et al., 1987). And then there is the question why this SD band shows such a good rotational spectrum; it deviates from the expression for a rigid rotor by only a few percent over the whole band. Is it a single unchanging configuration, or do a number of changing properties almost exactly cancel?

The evidence that this band involved a 2:1 deformation initially came entirely from the spacing between the lines in the spectrum, that is, from the magnitude of the moment of inertia, $\mathcal{J}$. The energy of a rigid rotor depends upon the square of the angular momentum, I, and inversely upon $\mathcal{J}$,

$$E = I(I + 1)\,\hbar^2/2\mathcal{J} \qquad (1)$$

For a doubly-even nucleus, I = 0,2,4..., and the difference between states is the experimentally determined γ-ray transition energy

$$E_\gamma = (4I - 2)\,\hbar^2/2\mathcal{J} \qquad (2)$$

If the nucleus were a rigid rotor, these would permit an experimental evaluation of $\mathcal{J}$. But the nucleus is not a rigid rotor, and does not follow eq. (1) exactly; for example, a Coriolis term must be added. This leads to the definition of more than one moment of inertia, e.g., a kinematic value, $\mathcal{J}^{(1)}$

$$\mathcal{J}^{(1)}/\hbar^2 = I/\omega \qquad (3)$$

and a dynamic one, $\mathcal{J}^{(2)}$

$$\mathcal{J}^{(2)}/\hbar^2 = dI/d\omega \qquad (4)$$

where

$$\hbar\omega = dE/dI = E_\gamma/2 \qquad (5)$$

The dynamic moment, $\mathcal{J}^{(2)}$ is a local (derivative) value most sensitive to changes in the nuclear configuration and properties, and since it does not depend upon the (not very well known) spin of the SD state (but only on the spin differential (dI = 2), it is the quantity most frequently compared with a calculated (deformed) moment of inertia. For the discrete SD band in ^{152}Dy, $\mathcal{J}^{(2)}$ varies only a few percent over the entire spin range and corresponds to an ellipsoid with an axis ratio of ~ 1.9, in agreement with theoretical expectations.

However, the moment of inertia is not always an accurate indicator of deformation; changes in pairing and in alignment also affect moments of inertia. In contrast, the nuclear quadrupole moment, Q_0, depends mainly on shape and deformation, and under certain assumptions it can be determined from the collective B(E2) of the band. The latter can be measured by a Doppler-shift attenuation method, DSAM. The Daresbury group carried out such a measurement, determining the centroid shifts for the SD band members in four forward (35°) and four backward (145°) detectors (Bentley et al., 1987). A plot of the resulting fractions of the full Doppler shift vs the upper spin of the transition is shown in Fig. 8. Calculated curves for several values of the quadrupole moment are also shown, assuming a constant Q_0 and no side-feeding. The latter assumption appears valid below I = 50, and the case for the former can be evaluated from the figure. A value of (19±3)b is indicated; this corresponds to a B(E2) of 2660 W.u. and an axial ratio of 1.9 for a uniformly charged ellipsoid as calculated from $Q_0 = (2/5)ZR^2[(c/a)^2 - 1]/(c/a)^{2/3}$. Thus the ~ 2:1 shape of the ^{152}Dy nucleus giving rise to this band

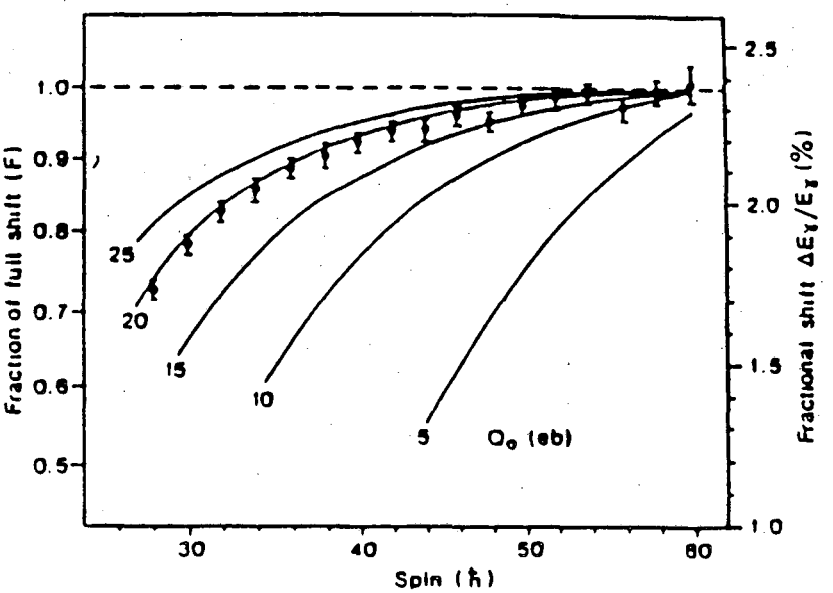

Fig. 8. Fraction of full Doppler shift of transitions in SD band. Curves are calculated for indicated values of the quadrupole moment (Bentley et al., 1987).

is confirmed.

There was almost a year before another SD band was found. It was in the odd-neutron nucleus ^{149}Gd and was found by the Canadian group using their newly completed "8π array" (Haas et al., 1988), and again consisted of a cascade of 19 transitions starting around spin 127/2 ħ. This was followed almost immediately by observation of a third SD band (Deleplanque et al., 1988), in ^{148}Gd, at Berkeley (Fig. 4). And this year the pace has speeded up still more with the discovery of four additional SD bands so far. These are in ^{150}Gd, ^{151}Tb, (Fallon et al., 1988), ^{151}Dy (Janssens et al., 1988), and ^{150}Tb, the first odd-odd example (Deleplanque et al., 1988a). A spectrum made up of the sum of spectra from double gates on ten of the SD lines in ^{150}Tb is shown in Fig. 9. In addition, there is a report of more than one discrete SD band in ^{146}Gd (Rzaca-Urban et al., 1988), but this case is less well characterized. All six of the new discrete SD bands have many features in common with the one in ^{152}Dy, and so the problems associated with it remain and are re-emphasized. Let me list them again.

1. Although the average intensity of the bands differ by small factors and do depend upon the production reaction, (mostly upon the maximum angular momentum and the initial excitation energy above that yrast SD band), they are of order 1% of the total yield of the product nucleus and ~20 times the extrapolated yield at spin 60 h for normal deformed

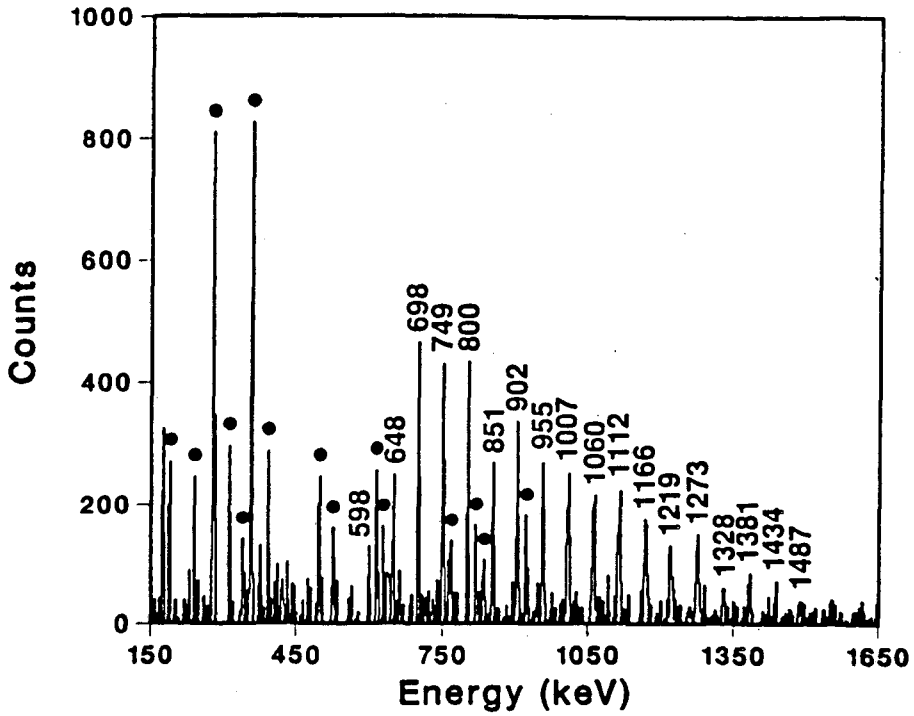

Fig. 9. Triple-coincidence spectrum summed on all double-gate combinations of ten SD lines in ^{150}Tb. The dots indicate known lines in coincidence with SD band (Deleplanque et al., 1988a).

bands in the rare earths.

2. The intensity in the band at first increases with decrease in spin, becomes roughly constant during the last half of the band, and then vanishes rapidly (two transitions). At its ending the SD band is several MeV above the yrast band (because of its larger moment of inertia).

3. No transitions linking the band to the yrast band that picks up its intensity have been observed, but the latter is reached over a small range of spin. As a result, neither the spins nor parity of the SD bands are accurately determined.

4. When the intensity from the SD band does reappear, it is in the yrast band and not spread over several bands, even when other bands appear to be more similar in shape to the SD band.

5. Only one discrete SD band is observed, although in the odd-mass examples one might expect to see the signature partner band as well. Excited continuum SD states do exist, however, as shown by the larger intensities usually observed for the appropriately spaced ridges in the two-dimensional coincidence matrices for these nuclei.

The kinematic moments of inertia, $\mathcal{J}^{(1)}$, for these bands, though not

well determined because of the inexact knowledge of the spins, appear to reach a high spin value of 83 $\hbar^2$ MeV^{-1}, which is only slightly smaller than expected for a rigid nucleus with a 2:1 axial ratio and is in agreement with the two quadrupole moment measurements (^{152}Dy, ^{149}Gd) that have been made. But the dynamic moments, $\mathcal{J}^{(2)}$, though large, are much more sensitive to the local changes in the nuclear structure and show a much wider variation as a function of rotational frequency ω, Fig. 10. Perhaps indicative of the importance of the shell gap in promoting the SD shapes, these observed bands are all in adjacent nuclei (however, this may only represent where they have been looked for most strenuously). Whatever the reason, it is a fortunate circumstance. For, if as is assumed in the simple Inglis cranking formula (Inglis, 1954), $\mathcal{J}^{(2)}$ is made up of additive contributions from

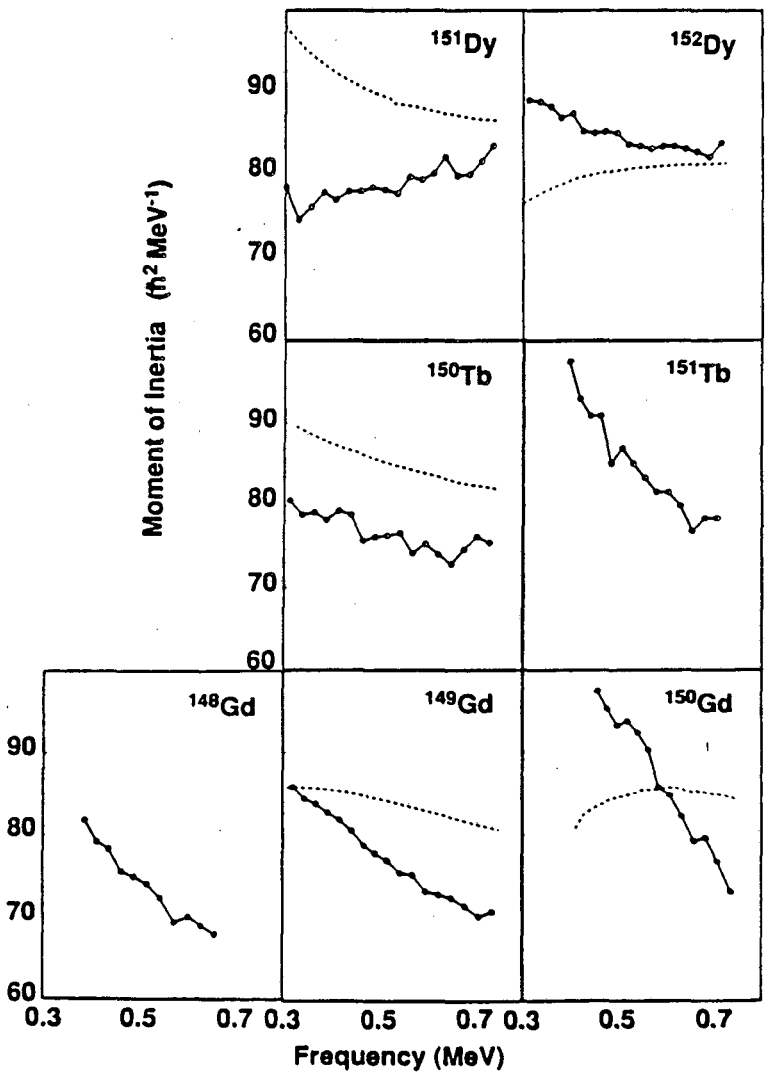

Fig. 10. Moments of inertia $\mathcal{J}^{(2)}$ (solid) and $\mathcal{J}^{(1)}$ (dotted) for the SD bands in the mass 150 region (Deleplanque et al., 1988a).

the constituent particles (with no account taken of changes in deformation or pairing), then the difference in moments of inertia of two neighboring nuclei should come from the additional nucleon. Since certain orbitals, in particular high-j intruder orbitals from one or even two shells above, can make large contributions to $\mathcal{J}^{(2)}$ at certain rotational frequencies, experimental observation of such contributions can then, in principle, be used to identify these orbitals and give the first experimental evidence for the nature of these SD configurations. For example, we can obtain the contribution to $\mathcal{J}^{(2)}$ from the 86th neutron in three ways: by subtracting the values of that moment for ^{151}Dy from those of ^{152}Dy; or those for ^{150}Tb from those for ^{151}Tb; or those of ^{149}Gd from the corresponding values for ^{150}Gd. These differences, $\Delta\mathcal{J}^{(2)}$, are plotted as solid lines in Fig. 11a and can be compared to the theoretical values shown in Fig. 11c. These latter curves (Åberg et al., 1988) represent the contribution to $\mathcal{J}^{(2)}$, as a function of $\hbar\omega$, of each of the first four individual proton orbitals in the $i_{13/2}$ subshell. They are obtained from the slopes of curves of $\langle j_x \rangle$ vs $\hbar\omega$ for these orbitals, which in turn are derived from the negative slopes of the single-particle energies in the rotating frame (Routhians) calculated as a function of ω. Since the behavior is rather similar for any intruder subshell, we may use this plot for comparison with both the neutron and proton experimental values, but must remember that they are not exactly the same. Furthermore, in this particular calculation of the Routhians, single best average values of the deformation parameters β_2 and β_4 and of the pairing gap Δ were used over the whole range of rotational frequency considered. These calculations suggest that the N=86 neutron corresponds to the second $j_{15/2}$ orbital, and therefore to curve 2 in Fig. 11c. Indeed, the decrease in $\Delta\mathcal{J}^{(2)}$ with rotational frequency for the experimental curves is in rough agreement with the calculated curve and consistent with identification of the N=86 neutron as the second $j_{15/2}$ orbital. However, the absolute magnitudes of the experimental curves differ from each other and from the calculated curve. Obviously either the N = 86 orbital differs somewhat in the three cases, or the cores are different, or both. Differences in the basic properties of the Dy, Tb, and Gd cores with the same number of neutrons, such as in their pairing correlations or shape and deformation are likely as a function of ω, but since the former are apt to be small at high spin, the latter are probably the

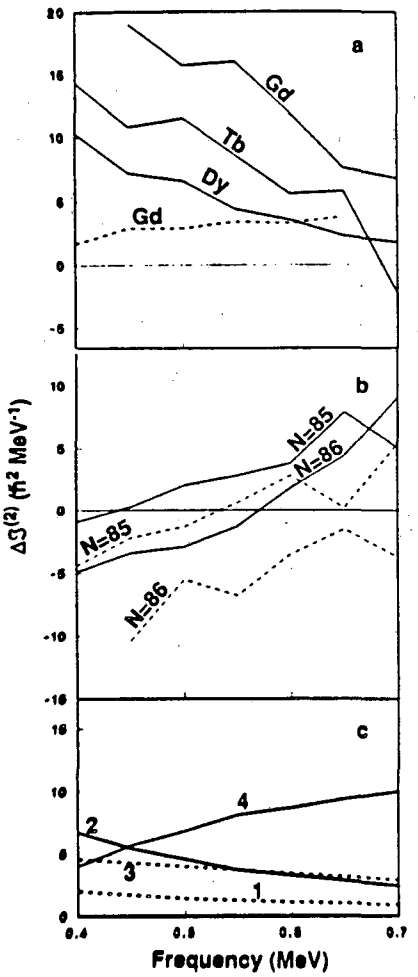

Fig. 11. (a) $\Delta\mathcal{J}^{(2)}$ for N = 86 (solid lines) and N = 85 (dashed line) obtained from the differences in the experimental moments, ^{152}Dy–^{151}Dy, ^{151}Tb–^{150}Tb, ^{150}Gd–^{149}Gd, and ^{149}Gd–^{148}Gd, respectively. (b) $\Delta\mathcal{J}^{(2)}$ for Z = 66 (solid lines) and Z = 65 (dashed lines) from ^{152}Dy–^{151}Tb, ^{151}Dy–^{150}Tb, and ^{151}Tb–^{150}Gd, ^{150}Tb–^{149}Gd, respectively. (c) Calculated values for $\Delta\mathcal{J}^{(2)}$ (Åberg et al., 1988) for the four lowest protons in the N = 6 shell (labeled 1, 2, 3, 4) with ε_2 = 0.556, ε_γ = 0.029 and γ = 0°.

cause. The resulting small changes in the cores and in the orbitals themselves, as well as in the core-orbital interaction (polarization), may make 5-10% differences in the moments of inertia not unreasonable (see below).

Similarly, the contribution of the 85th neutron can be obtained by subtracting the moments of inertia for ^{148}Gd from those for ^{149}Gd, and this is shown as a dashed line in Fig. 11a. Such a flat (slightly rising) curve is not in disagreement with the calculated curve 1 (slightly falling) of Fig. 11c, but is not very significant, as the calculations suggest that the 85th orbital in this case might be a low-j orbital

which would also give a flat contribution in this frequency range. Thus one cannot differentiate between these possibilities.

By subtracting the values of ^{150}Tb from those of ^{151}Dy, and those of ^{151}Tb from those of ^{152}Dy, we can likewise obtain the experimental contribution of the Z=66 proton to $\mathcal{J}^{(2)}$. And by subtracting the values for ^{150}Gd from those of ^{151}Tb, and those of ^{149}Gd from those of ^{150}Tb, we can determine two curves for the Z=65 proton. These are plotted in Fig. 11b. The calculations suggest that these should be the fourth and third $i_{13/2}$ proton orbitals, respectively. Curve 4 in this frequency range is calculated to increase (Fig. 11c), in agreement with experiment. But the third orbital is calculated to remain flat (slightly decreasing), in contradiction to the experimental curves. And within each pair, the curves have different magnitudes, also in contradiction to our expectation of a unique behavior for each last orbital. The reasons for these differences are probably those given two paragraphs above for the neutron orbitals. Indeed, for ^{150}Gd and ^{151}Tb I have been shown at this school the results of better calculations of $\mathcal{J}^{(2)}$ vs ω which are self-consistent, in that they minimize the particle energies at increasing values of ω with respect to β_2 and β_4, rather than using constant (average) values over the whole frequency range, and also employ values of Δ which decrease with ω, a more realistic assumption than using a constant (initial) value (Nazarewicz, 1988). By accident, the experimental difference, $\mathcal{J}^{(2)}$, for these two nuclei (Fig. 11b) gives the poorest comparison of any with the calculated curves in Fig. 11c. But the new calculations are in much better agreement, even to the extent of yielding a negative, but rising, curve of $\Delta\mathcal{J}^{(2)}$. (This results from a band crossing at the beginning of the frequency interval in the new calculations for ^{150}Gd which makes the moment unusually large, as is seen in the experimental values). We feel that these results are a promising start to a new moment-of-inertia spectroscopy of the SD bands and the best way at present to determine their configuration. As the systematics of SD bands grows and the calculations become more complete, these attempts to determine the contribution of the last (high-j) orbital (presumably one of those responsible for the SD shape itself) to the moment of inertia will also become more refined and will better help to understand their structure.

In this second lecture, I would like to describe some results in another region of the Periodic table, the mass 130 region. In actual fact, the

first observation of an unusual band indicating large deformation was not in ^{152}Dy, but in ^{132}Ce. This was published in 1985 by a group at Daresbury (Nolan et al., 1985), and, if one adopts a generalized definition of superdeformed as a band with larger than normal deformation, this would be the first example outside the actinide region. As with the mass 150 SD bands already described, no transitions were found connecting the bottom of the new band with the yrast band, so that spins were not determined to better than ± 2 $\hbar$. The moments of inertia indicated a deformation of ε=0.35-0.4, roughly corresponding to an axial ratio 3:2. To provide a more unambiguous determination of the deformation, a measurement of the quadrupole moment was carried out last year by a Doppler-shift centroid experiment with a gold-backed target (Kirwan et al., 1987). Again the necessary assumptions were a constant deformation for the whole band and no side-feeding, and again the first assumption appears reasonable from the reasonable fit of the data to the calculated curves. The second assumption, though wrong, has little effect since the feeding appears to be relatively fast and occurs only at the highest spins which are not very sensitive for this measurement. The quadrupole moment so determined, Q_0=8.8b, corresponds to $\varepsilon \sim 0.4$, in agreement with the moments of inertia.

Then last year, another strongly deformed band was found in this mass region, in ^{135}Nd, using HERA (Beck et al., 1987). At the time it was the first odd-mass case. The spectrum obtained as the sum of double-gated spectra, with one gate on an in-band transition and the other either on a second in-band line or on a coincident low-lying transition, is shown in Fig. 12. All of the lines in the figure are in ^{135}Nd and those of the band are labeled with their energies. Transitions marked with an # are in the ground band and those marked with a short vertical line are possible connecting transitions between the new band and low-lying bands. This is still the only example among the seven mass 150 and eight mass 130 bands now known where such linking transitions have been seen. This lack of observation is quite likely due to the fact that these bands decay out rather suddenly via a rather large number of paths, none of which are intense enough to be seen. Because the bottom of the band in ^{135}Nd has ~ 10% of the total intensity of that product (rather than the 0.5-2% of the mass 150 examples), the strongest pathways can be seen. But even so, the four paths indicated in the decay scheme of Fig. 13 account for only a little more than half of the band

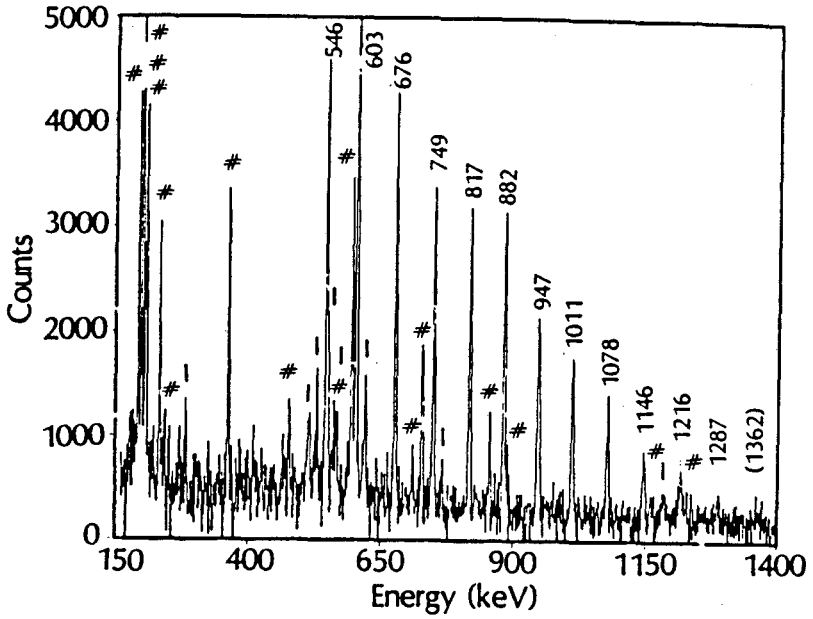

Fig. 12. Double-gated spectrum of SD transitions in ^{135}Nd labeled by energies. See text (Beck et al., 1987).

intensity. There remains ~ 40% of the band intensity that must go by > 4 transitions to reduce their individual intensities to < 1% of that of the product nucleus and thus be too small to be seen. It is not understood why all these bands should decay in so many ways, rather than to the one band most similar in configuration.

In the last year and a half, the pace of discovery of new bands in this region has also speeded up; six more examples have been found. The doubly-even nuclei ^{134,136}Nd showed bands (Beck et al., 1987a), as did the odd-neutron nuclei ^{133,137}Nd (Wadsworth et al., 1987), giving five neighboring nuclei in a row. It will be interesting to compare the dependence of their moments of inertia on the last neutron in each case, but the calculations have not yet been completed. This year two more bands have been seen in ^{131}Ce (Luo et al., 1988) and ^{130}La (Nolan et al., 1988), and it seems probable that still more may be found in this region. Although none of these mass 130 bands have been studied and characterized as well as ^{152}Dy, some general comments can be made about them, and because of the great intensity of some of them (20% of the total product yield for ^{133}Nd), it is hoped that the transitions linking the new band and the low-lying bands can be found and that their properties and the nature of their configurations can be determined. In general the dynamic moments of inertia of the mass 130 bands are similar to each other. They fall more steeply with rotational frequency than

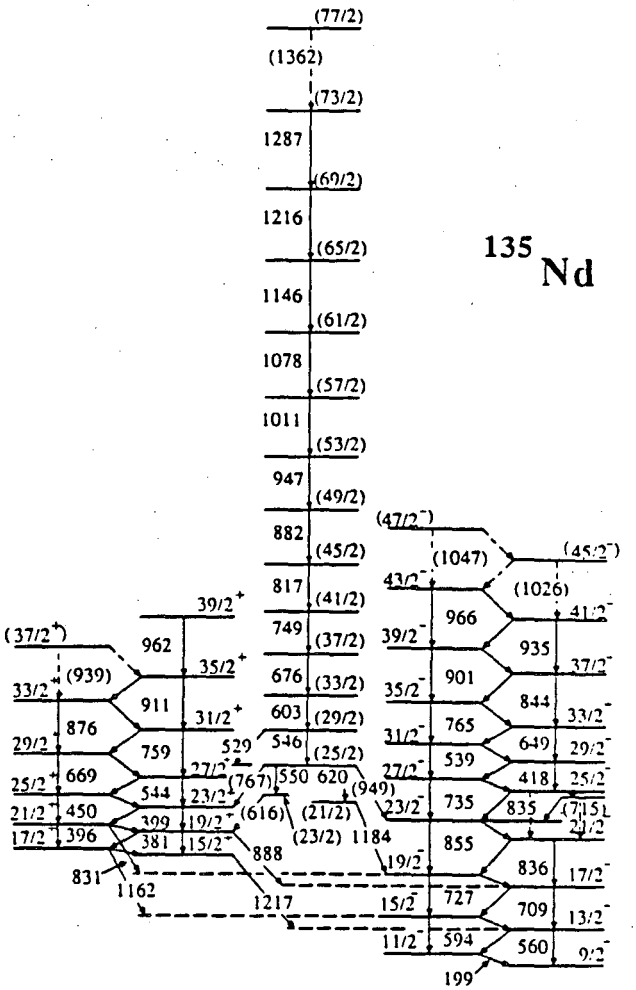

Fig. 13. Level scheme of ^{135}Nd (Beck et al., 1987).

those of the mass 150 region, tend to show a bump at intermediate frequencies which may be due to a band crossing with a moderate mixing matrix element, and most of them show an irregularity at the bottom of the band which is likely a band crossing with a smaller matrix element. One of them, ^{137}Nd shows a sharp increase just above a frequency of 0.5 MeV which certainly looks like a crossing, and if so, would be the first marked one observed. The more rapid decrease in $\mathcal{J}^{(2)}$ with ω, the greater irregularity in the bands, and the smaller deformation all suggest a smaller influence from high-j orbitals, e.g., a smaller number of them, and/or orbitals from one shell above rather than two. Two more features of these mass 130 bands can be noted; the odd-mass Nd bands are more intense than those of the even nuclei, and the band in ^{135}Nd appears to lie lower than those in ^{134,136}Nd, although the excitation energies at the bottom of the bands in the latter are not well determined. Actually, the first property may be just a reflection of the

second one. And the latter may indicate that pairing is much reduced in the SD bands relative to the yrast band, in both odd and even nuclei. This seems reasonable theoretically, but it would be very interesting to determine this question experimentally. Unfortunately, we may have to wait for still more sensitive Ge arrays to be able to pick out some of the de-exciting pathways in the even nuclei to settle this.

Because the bands in the Nd nuclei have about the same moments of inertia as those in ^{132}Ce, it was assumed that the deformation of the Nd nuclei was also about the same and involved an axial ratio of ~ 1.5. But we decided to be on the safe side and to determine the quadrupole moment of the band in ^{135}Nd by a DSAM measurement, that is, by determining the lifetimes of the strongly deformed states from the Doppler-shift of their transitions as the recoil nuclei slowed down in the ^{100}Mo target and its thick gold backing. That these transitions are fast compared to the stopping time can be seen in Fig. 14, where the upper spectrum is from four Ge detectors in the backward hemisphere at ~ 150° and the lower spectrum is from four Ge detectors at 42°. As the cascade proceeds down the band to lower spins and transition energies, the Doppler shift becomes a smaller fraction of the full shift corresponding to the initial recoil velocity. Making the two assumptions of assigning the SD band a constant Q_0 and assuming no effect from side-feeding, curves of the fractional Doppler shift, or of v/c, can be calculated for different values of Q_0 and compared with the experimental results. This is done in Fig. 15, where the experimental points indicate a Q_0 of (6.5 ± 1.0)b. This was a surprise, being significantly below the value of 8.8 barns found for ^{132}Ce, in spite of the similar $\mathcal{J}^{(2)}$ values. However, the shifted spectra contain more information than has been used in determining the centroids of the transitions; one can look at the lineshapes of the transitions, and if there are sufficient statistics and not too much interference from other lines, a comparison can be made with a Monte Carlo calculation of the lineshapes. An example is given in Fig. 16 of one of the more striking cases. Shown for the 882 keV, 49/2 → 45/2 transition in the four backward detectors are the experimental line shape, that calculated for Q_0=6.5b with no side-feeding, and the lineshape calculated for Q_0=8.6b but allowing for the measured side-feeding (the difference in the intensity from the preceding main-band transition) as a cascade of five transitions with the energies of the five main-band transitions above the transition of interest and a fixed

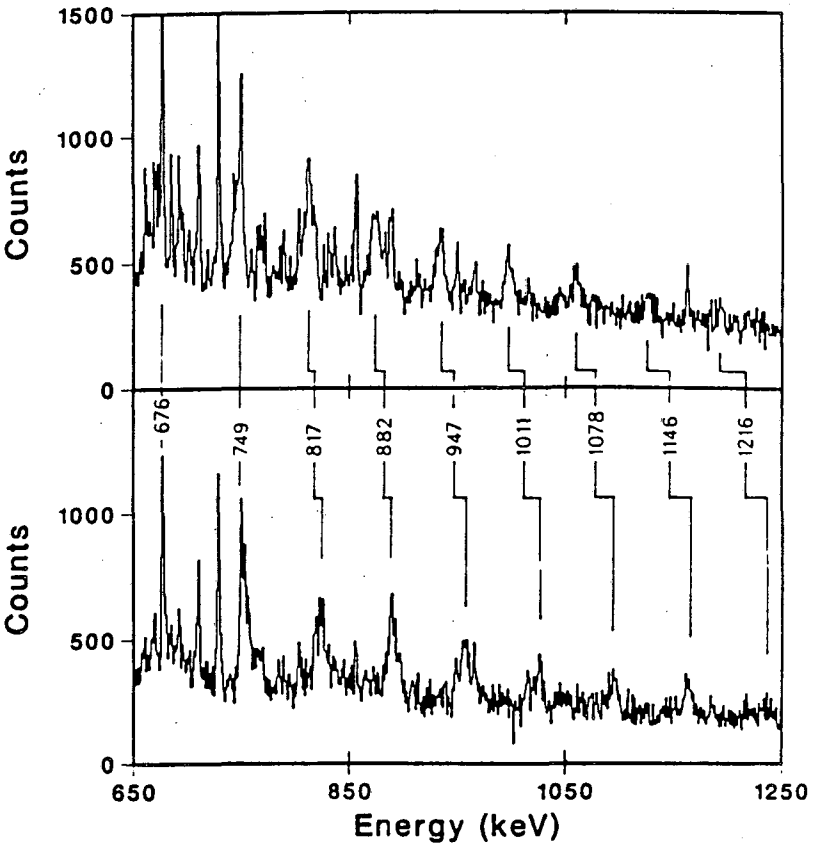

Fig. 14. Backward and forward Doppler-shifted spectra of ^{135}Nd.

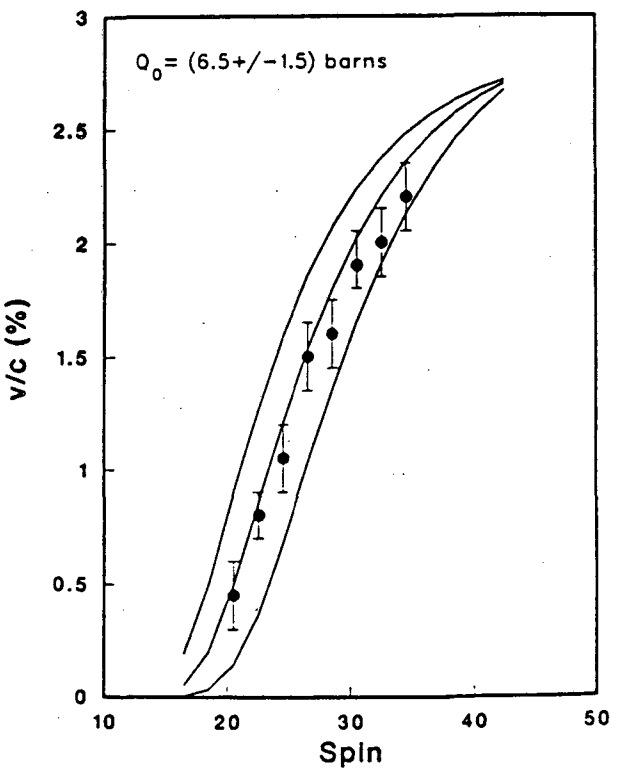

Fig. 15. Plot of v/c vs upper spin of transition for spectra of Fig. 14. Calculated curves for Q_0=(6.5±1.5)b and no side feeding.

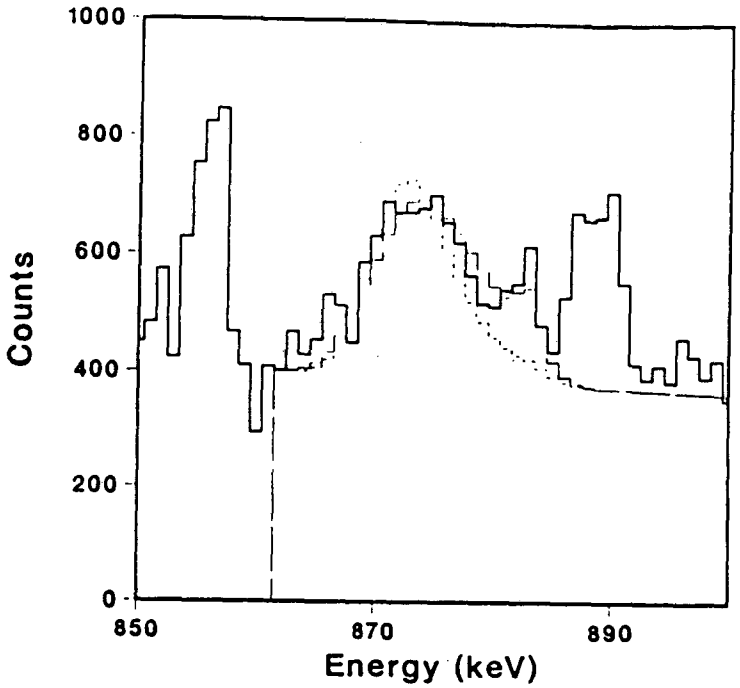

Fig. 16. Solid line is the lineshape of the 882 keV transition in the SD band of ^{135}Nd from the backward detectors. The short-dashed curve is calculated for Q_0=6.5b and no side-feeding, and the long dashed curve is for Q_0=8.6b and slow side-feeding. (See text.)

quadrupole moment of 1.8b. These two moment values give the best simultaneous fit to the lineshapes of the 10 transitions considered, both for forward and backward groups of detectors, and it can be seen in Fig. 16 that a stopped peak is adequately produced by the slower component introduced by the side-feeding. Figure 17 shows that the resulting calculated centroid curve gives a better fit to the data than the curves in Fig. 15. But the curve of χ^2 obtained fitting the lineshapes with different values of Q_0 for the main and side-feeding bands has a shallow minimum, so that there remains considerable uncertainty in the value of the main-band quadrupole moment, Q_0=(8.6 ± 1.0)b. The reason for the difference with the ^{132}Ce case is that the sidefeeding in ^{135}Nd extends all the way down to the bottom of the band, and thus the slow side-feeding has a chance to be felt in the successive decays. In the three previous measurements, side-feeding occurred only in the first half of the band and appeared to be quite fast itself. It does appear, however, that the ^{135}Nd quadrupole moment, and hence its deformation, is most likely quite similar to that in ^{132}Ce, as originally expected. But it is also clear that care must be exercised in using the centroid only DSAM measurements, particularly if there is slow side-feeding.

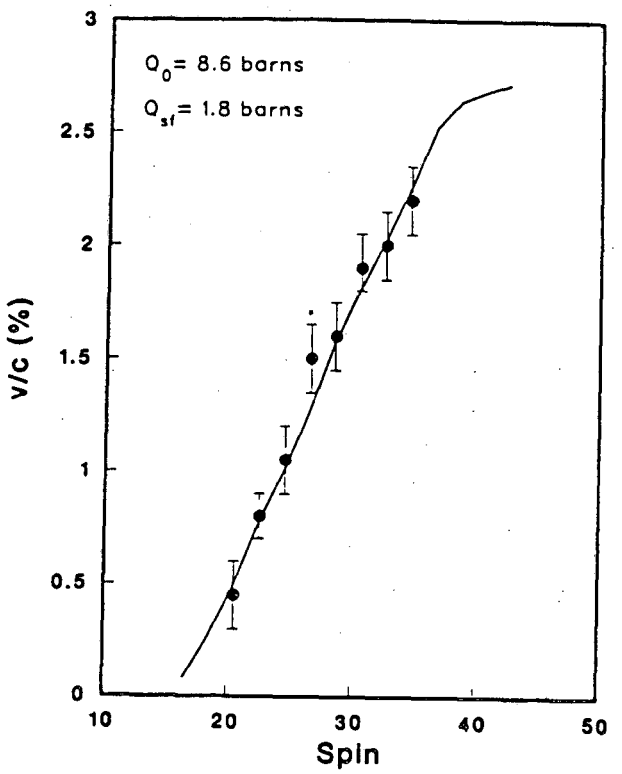

Fig. 17. Plot of v/c vs upper spin of ^{135}Nd SD transtions. Curve is calculated for Q_0=8.6b and slow side-feeding, as described in text.

I would like to add one additional comment to the SD band story in the mass 130 region. If it is found generally that the odd-mass bands do lie lower than the even ones, that is, closer to the ground band by an MeV or so, as mentioned earlier on the properties of the ^{135}Nd band, a likely explanation is that there is little pairing left in the SD bands. Is there any (other) indication of this? Bohr and Mottelson (1975a) give an expression relating the ratio of the kinematic moment of inertia to that of a rigid ellipsoid as a function of the deformation parameter δ divided by the pairing gap parameter Δ,

$$\mathcal{J}^{(1)}/\mathcal{J}_{rigid} = [1 - g\,(\frac{\hbar\omega_0\delta}{2\Delta})]$$

$$g(x) = \frac{\ln\,[x + (1 + x^2)^{1/2}]}{x(1 + x^2)^{1/2}} \qquad (6)$$

and $\hbar\omega_0$ is the spherical shell spacing, $41/A^{1/3}$ MeV. Such an expression gives the right order of magnitude for $\mathcal{J}^{(1)}/\mathcal{J}_{rigid}$ in the ground-band states of even nuclei for values of Δ and δ determined from odd-even mass differences and quadrupole moments, respectively, as shown in Fig. 18 for $2^+ \rightarrow 0^+$ transitions in nuclei from ^{82}Se to ^{238}U. Also plotted are points for the SD bands in ^{152}Dy, ^{149}Gd,

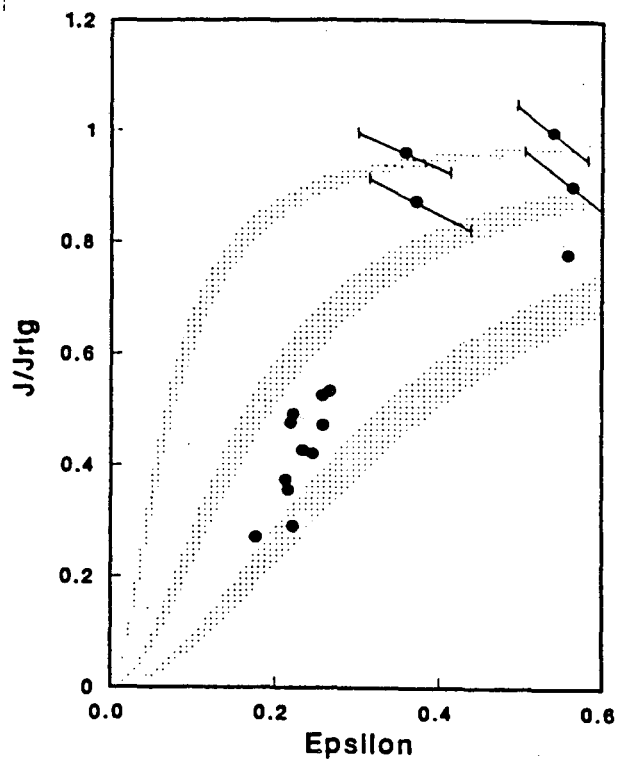

Fig. 18. Plot of $\mathcal{I}^{(1)}/\mathcal{I}_{rigid}$ vs deformation parameter ε. Dotted regions are for pairing gap parameter (Δ) values of 1.0, 0.5, and 0.2 MeV, reading upwards. The cluster of points at ε=0.2-0.3 are from normally deformed nuclei, from ^{82}Se to ^{238}U. The two points at ε=0.38 are for SD transitions in ^{132}Ce and ^{135}Nd, reading upwards, and those at ε~0.6 are for SD transitions in ^{240}Pu, ^{152}Dy, and ^{149}Gd.

^{240}Pu, and ^{132}Ce and ^{135}Nd. It can be seen that the four rare-earth bands, in contrast to the normally deformed 2^+ states, all fall near the Δ = 0.2 MeV curve, suggesting a strong reduction in the pairing correlations for these high-spin SD states (that is, if eq. (6) still has sufficient validity at such large deformations). On the other hand, the low-spin SD band in ^{240}Pu falls between the 1.0 and 0.5 MeV curves, more like the normal bands, as was expected.

I hope this brief, somewhat fragmentary account of the present status of SD bands gives you a taste of the excitement and activity in this field at this time, and convinces you that although we have learned something about them, what we don't know is much greater. We can look forward to even more interesting results, including, perhaps, the observation of hyperdeformed 3:1 shapes. The development of still more powerful arrays such as GAMMASPHERE and Euroball will surely take us into new fields of exploration and promise an exciting future.

Acknowledgments: I am indebted to a number of enthusiastic workers at the Lawrence Berkeley Laboratory for help, ideas, and data in preparing these lectures. They performed the work I have described as coming from here; they are Marie-Agnès Deleplanque, Frank Stephens, José Bacelar, Con Beausang, Eva-Maria Beck, Jacob Burde, Jim Draper, Cemal Duyar, Augusto Macchiavelli, and Dick McDonald.

REFERENCES

Åberg, S., et al. 1988, XXVI International Winter Meeting on Nuclear Physics, Bormio, Italy
Beck, E.M., et al. 1987, Phys. Rev. Lett. 58, 2182
Beck, E.M., et al. 1987a, Phys. Lett. B195, 531.
Bentley, M.A., et al. 1987, Phys. Rev. Lett. 59, 2141.
Bohr, A. and Mottelson, B., 1975, Nuclear Structure, vol. II (W.A. Benjamin, Inc., Reading, MA), p. 622.
Bohr.A. and Mottelson, B. 1975a, ibid., p. 82.
Deleplanque, M.A., et al. 1988, Phys. Rev. Lett. 60, 1626.
Deleplanque, M.A., et al. 1988a, preprint, LBL-25941
deVoigt, M.J.A., et al. 1987, Phys. Rev. Lett. 59, 270.
Diamond, R.M. and Stephens, F.S. 1981, "The High Resolution Ball" (proposal, unpublished); Diamond, R.M., "The Berkeley High Resolution Ball,"Instrumentation for Heavy-Ion Research (Harwood Academic Pub., New York, 1985), p. 259.
Dudek, J. et al. 1987, Phys. Rev. Lett. 59, 1405.
Fallon, P., et al. 1988, Slide report, Workshop on Nuclear Structure, Copenhagen
Haas, B., et al. 1988, Phys. Rev. Lett. 60, 503.
Inglis, D.R. 1954, Phys. Rev. 96, 701.
Kirwan, A.J., et al. 1987, Phys. Rev. Lett. 58, 467.
Luo, Y.-X., et al. 1988, Z. Phys. A329, 125.
Nazarewicz, W. 1988, private communication.
Neergaard, K., et al. 1976, Nucl. Phys. A262, 61.
Nolan, P.J., et al. 1985, J. Phys. G: Nucl. Phys. 11, L17.
Nolan, P.J., et al. 1988, reported in Slide report, Workshop on Nuclear Structure, Copenhagen.
Nyako, B.M. et al. 1984, Phys. Rev. Lett. 52, 507.
Polikanov, S.M., et al. 1962, Soviet Physics JETP 15, 1016.
Ragnarsson, I., et al. 1980, Nucl. Phys. A347, 287.
Strutinski, V.M., 1967, Nucl. Phys. A95, 420.
Twin, P.J., et al. 1986, Phys. Rev. Lett. 57, 811.
Wadsworth, R. et al. 1987, J. Phys. G: Nucl. Phys. 13, L207.

LAWRENCE BERKELEY LABORATORY
TECHNICAL INFORMATION DEPARTMENT
UNIVERSITY OF CALIFORNIA
BERKELEY, CALIFORNIA 94720